

Studies of Distortional Isomers: Spectroscopic Evidence That Green *cis,mer*-Dichlorotrakis(dimethylphenylphosphine)oxomolybdenum(IV) Is a Mixture

Patrick J. Desrochers,^{1a} Kenneth W. Nebesny,^{1a} Michael J. LaBarre,^{1a}
Sandra E. Lincoln,^{1b,c} Thomas M. Loehr,^{1b} and John H. Enemark*,^{1a}

Contribution from the Department of Chemistry, University of Arizona, Tucson, Arizona 85721, and Department of Chemical and Biological Sciences, Oregon Graduate Institute of Science & Technology, Beaverton, Oregon 97006-1999. Received June 17, 1991

Abstract: The blue (1) and green (2) forms of *cis,mer*-MoOCl₂(PMe₂Ph)₃ are not distortional isomers. An authentic sample of green 2 has been chromatographically and spectroscopically characterized to be a 65:35 mole fraction mixture of blue *cis,mer*-MoOCl₂(PMe₂Ph)₃ and yellow *mer*-MoCl₃(PMe₂Ph)₃ (yellow 3), respectively. Thin-layer chromatography separates green 2 into two individual peaks due to blue 1 and yellow 3. Elemental analysis of green 2 shows a significantly higher percent chlorine relative to blue 1, consistent with the presence of a 0.35 mole fraction of yellow 3 in green 2. Both infrared (500–150 cm⁻¹) and Raman (1625–125 cm⁻¹) spectra of green 2 have distinct features due to contributions from blue 1 and yellow 3. Furthermore, Raman spectra of blue 1 and green 2 indicate a $\nu(\text{Mo}=\text{O})$ band at $944 \pm 1 \text{ cm}^{-1}$ that is conspicuously absent in the spectrum of yellow 3. The 500-MHz ¹H NMR spectrum for green 2 shows several resonances characteristic of paramagnetic yellow 3 in the regions +7.5 to +11.5 ppm and -22 to -41 ppm. Visible spectroscopy implies that the color of green 2 is due to the summation of absorptions from blue 1 and yellow 3. X-ray photoelectron spectroscopy (XPS) of the Mo 3d regions resolves the contributions from the Mo(IV) (blue 1) and Mo(III) (yellow 3) species in green 2. Both the visible and XPS results confirm the 65:35 (blue 1:yellow 3) molar composition of green 2. The facile cocrystallization of blue 1 and yellow 3 to give green 2 is likely driven by the increased entropy of the green 2 crystals, which decreases the free energy of crystallization. Similar compositional disorder processes are probably responsible for the anomalous bond lengths ascribed to distortional (bond stretch) isomerism in other series of inorganic complexes.

Introduction

Distortional isomerism was first proposed¹ to explain the blue (1) and green (2) forms observed² for *cis,mer*-MoOCl₂(PMe₂Ph)₃. X-ray structural analyses of blue 1⁴ and green 2⁵ revealed that the green species appeared to have a significantly longer Mo=O bond (1.80 Å) versus the more typical value⁶ of 1.68 Å found for the blue form. Since the first report of this "possibility of a new type of isomerism" in 1971,³ several other examples of distortional isomers have been claimed.⁷⁻⁹ Wiegardt and Backes-Dahmann reported the preparation and characterization of the blue and green forms of [LWOC₂]PF₆ (L = 1,4,7-trimethyl-1,4,7-triazacyclononane) in 1985.⁷ Two of the most recently proposed examples include series of compounds of the form M(E)X₃(PMe₂)₃ (M = Nb, Ta; E = O, S; X = Cl, Br).⁸ These sulfur-containing compounds represent the first assertion of distortional isomerism in a metal-sulfido unit. All but one⁹ of these cases offer crystallographic evidence that two differently colored compounds can

have the same molecular formulas and stereochemistries but exhibit significantly disparate metal-oxo or metal-sulfido bond lengths, with one form (usually the green) having an anomalously long metal-oxo or -sulfido bond. In addition to this body of experimental evidence, an extensive theoretical rationalization for the existence of distortional isomers has been developed.¹⁰ Therefore, it is interesting that Parkin and co-workers recently showed¹¹ that adding increasing amounts of yellow *mer*-MoCl₃(PMe₂Ph)₃ (yellow 3) to blue 1 yielded green crystals with a continuum of increasing Mo=O bond lengths. Here we show by independent spectroscopic techniques that the green "isomer" of Butcher and Chatt's original reports² is really an intimate mixture of blue 1 and yellow 3.¹² Some of the implications that these results may have for other proposed distortional isomers are also discussed.

Experimental Section

Blue and green MoOCl₂(PMe₂Ph)₃² and yellow MoCl₃(PMe₂Ph)₃¹³ were synthesized according to literature methods except that MoCl₄(NCMe)₂¹⁴ was used in place of MoCl₄(NCEt)₂. Molybdenum pentachloride and dimethylphenylphosphine were obtained from Aldrich Chemicals and used as received. Elemental analyses were performed by Atlantic Microlabs, Norcross, GA. Thin-layer chromatography was run on silica gel plates (Analtech silica gel GF; 250- μm layer thickness) using 95:5 toluene/acetonitrile as eluent.

Spectroscopy. All spectra were obtained at room temperature unless otherwise noted.

Infrared. Full spectra (4000–300 cm⁻¹) were obtained from samples in KBr wafers using a Perkin-Elmer Model 983 spectrometer. Low-en-

(1) (a) University of Arizona. (b) Oregon Graduate Institute. (c) Present address: Department of Physical and Life Sciences, University of Portland, Portland, OR 97203.

(2) Butcher, A. V.; Chatt, J. J. *Chem. Soc. A* 1970, 2652.

(3) Chatt, J.; Manojlović-Muir, L.; Muir, K. W. J. *Chem. Soc. D* 1971, 655.

(4) Manojlović-Muir, L. J. *Chem. Soc. A* 1971, 2796.

(5) Haymore, B. L.; Goddard, W. A., III; Allison, J. N. *Proc. Int. Conf. Coord. Chem.*, 23rd 1984, 535. Apparent unresolvable disorder between two Mo positions precluded full publication of this study (B. Haymore, private communication).

(6) (a) Mayer, J. M. *Inorg. Chem.* 1988, 27, 3899. (b) Nugent, W. A.; Mayer, J. M. *Metal-Ligand Multiple Bonds*; Wiley Interscience: New York, 1988.

(7) (a) Backes-Dahmann, G.; Wiegardt, K. *Inorg. Chem.* 1985, 24, 4049. (b) Wiegardt, K.; Backes-Dahmann, G.; Nuber, B.; Weiss, J. *Angew. Chem., Int. Ed. Engl.* 1985, 24, 777.

(8) (a) Bashall, A.; McPartlin, M. *Acta Crystallogr.* 1990, 46A, C-221. (b) Gibson, V. C.; Kee, T. P.; Shaw, A.; Williams, D. N. *Abstracts of Papers*, 199th National Meeting of the American Chemical Society, Boston, MA; American Chemical Society: Washington, DC, 1990; INOR 134. (c) Bashall, A.; Gibson, V. C.; Kee, T. P.; McPartlin, M.; Robinson, O. B.; Shaw, A. *Angew. Chem., Int. Ed. Engl.* 1991, 30, 982.

(9) Degnan, I. A.; Behm, J.; Cook, M. R.; Herrmann, W. A. *Inorg. Chem.* 1991, 30, 2165.

(10) (a) Yves, J.; Lledos, A.; Burdett, J. K.; Hoffmann, R. J. *Am. Chem. Soc.* 1988, 110, 4506. This paper describes blue 1 and green 2 as "bond stretch isomers". (b) Subsequent to the submission of this paper, we learned that recent ab initio calculations indicate that only one stable isomer should exist for the [LWOC₂]⁺ and *cis,mer*-MoOCl₂(PMe₂Ph)₃ systems: Song, J.; Hall, M. B. *Inorg. Chem.*, in press.

(11) Yoon, K.; Parkin, G.; Rheingold, A. L. *J. Am. Chem. Soc.* 1991, 113, 1437.

(12) Presented in part at the 201st National Meeting of the American Chemical Society, Atlanta, GA, April 14, 1991; see Abstract INOR 50.

(13) Anker, M. W.; Chatt, J.; Leigh, G. J.; Wedd, G. A. *J. Chem. Soc., Dalton Trans.* 1975, 2639.

(14) Dilworth, J. R.; Richards, R. L. *Inorg. Synth.* 1980, 20, 119.

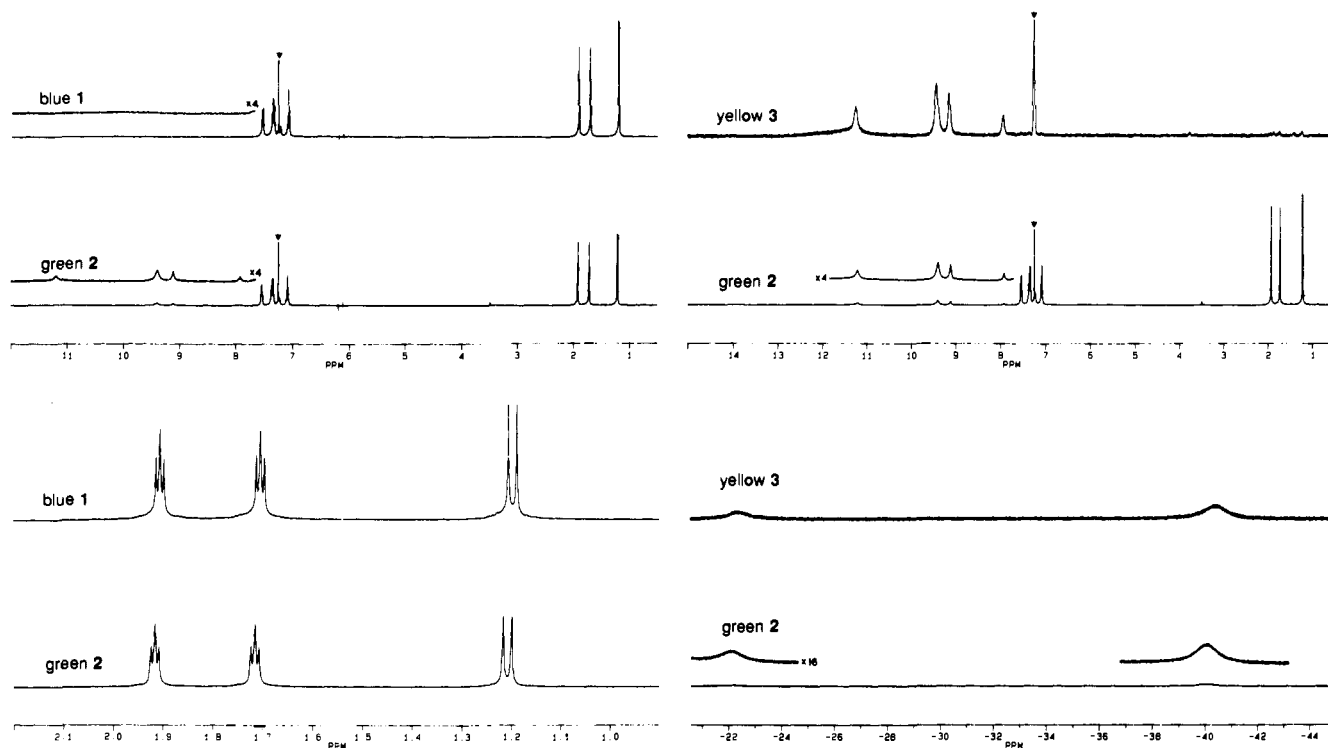


Figure 1. 500-MHz ^1H NMR spectra: (A, top left) blue 1 and green 2 (6494-Hz sweep width) spectra ($\nabla = \text{CHCl}_3$) with the four weak broad resonances in the 7.8–11.8 ppm region of the green 2 spectrum assigned to yellow 3; (B, bottom left) closeups of the methyl proton regions from spectra of blue 1 and green 2 where the pattern of two triplets and one doublet (1:1:1 relative intensity) has been assigned previously^{16,17} and is indicative of the configuration *cis,mer*- $\text{MOX}_2(\text{PMe}_2\text{Ph})_3$; (C, top right) spectra of green 2 and paramagnetic yellow 3 (41 666- and 33 333-Hz sweep widths, respectively) ($\nabla = \text{CHCl}_3$) showing their common peaks in the downfield chemical shift region; (D, bottom right) spectra of green 2 and paramagnetic yellow 3 showing their common peaks in the upfield chemical shift region.

ergy spectra (150–500 cm^{-1}) were run on a Perkin-Elmer Model 1800 FT-IR spectrometer for samples as Nujol mulls smeared onto thin (ca. 0.5 mm thick) silicon plates.

Raman. Spectra (125–1625 cm^{-1}) were recorded at 90 K using 514.5-nm excitation radiation on a computerized Jarrell-Ash 25-300 spectrophotometer equipped with a Spectra-Physics Model 164 Ar ion laser, a cooled RCA C31034 photomultiplier, and an ORTEC Model 9302 amplifier/discriminator. Solid samples were sealed under nitrogen in glass capillaries.

Proton NMR. Each spectrum was run on a Bruker AM 500-MHz spectrometer at the ambient probe temperature of 22 $^\circ\text{C}$ using a block size of 64 kbytes. A 30 $^\circ$ pulse width and no line broadening were used. Blue 1, green 2, and yellow 3 spectra were the result of 160, 160, and 64 scans, respectively. All of the resonances were accounted for in the region +40 to –60 ppm; however, optimum sweep widths were used (see Figure 1) for the best resolution in individual spectra. Deuterated chloroform refluxed and distilled over phosphorus pentoxide was used as the solvent, and each sample was prepared (ca. 50 mM) and run under a nitrogen atmosphere. The proton chemical shifts were internally referenced to residual CHCl_3 protons at 7.24 ppm.

UV-Visible Electronic. Samples were run under a nitrogen atmosphere in acetonitrile that had been refluxed and distilled over calcium hydride. A Cary 14 spectrometer equipped with an On-Line Information System (OLIS) data acquisition system and 1.0-cm quartz cells were used to record the spectra from 800 to 300 nm.

X-ray Photoelectron. Instrumental details are described elsewhere.¹⁵ Mg $K\alpha$ radiation was used on solid samples pressed into indium foil. Reported binding energies are referenced relative to the carbon 1s peak at 284.6 eV to correct for differences due to charging effects within individual samples. Spectra were run at ca. –150 $^\circ\text{C}$ to inhibit sample degradation.

Spectroscopic results are summarized in Tables II–VII, with representative spectra in Figures 1 and 3–6.

Results and Discussion

Chemical Analyses. Authentic samples of blue and green $\text{MoOCl}_2(\text{PMe}_2\text{Ph})_3$ were prepared using the previously published procedure.² Their elemental analyses and ^1H NMR and infrared

Table I. Elemental Analysis Data for $\text{MoOCl}_2(\text{PMe}_2\text{Ph})_3$ ($\text{C}_{24}\text{H}_{33}\text{Cl}_2\text{OMoP}_3$, Fw = 597.33)

		% C	% H	% Cl
calcd		48.25	5.58	11.87
found		Blue 1		
	this work	48.18	5.50	11.68
	ref 2	48.5	5.9	12.1
		Green 2		
	this work	47.52	5.51	12.72
	ref 2	48.0	5.5	12.7

spectra were consistent with those originally reported.² However, each of the following detailed characterizations supports the conclusion¹¹ that green 2 is an intimate mixture of blue 1 and yellow 3, rather than a purported “distortional isomer” of blue 1.³

Thin-layer chromatography (TLC) of blue 1 in toluene/acetonitrile (95:5) showed a single, essentially immobile brown spot. The TLC of yellow 3 gave a single yellow spot with an R_f value of about 0.7. Green 2 separated into two bands corresponding to the brown spot of pure blue 1 and the more mobile yellow spot of pure yellow 3. These results provide strong evidence that green 2 is actually a mixture of blue 1 and yellow 3. Surprisingly, chromatographic analysis has not been previously reported in the investigation of distortional isomers.

Elemental analyses of the present blue and green forms of $\text{MoOCl}_2(\text{PMe}_2\text{Ph})_3$ provided additional evidence that the green form is a mixture. If blue 1 and green 2 were distortional isomers, they would have identical molecular formulas and should have given the same analyses. Yet our green 2 was much higher in percent chlorine compared to blue 1 and theory (Table I). A similar discrepancy was also observed in the original analysis of the green form of $\text{MoOCl}_2(\text{PMe}_2\text{Ph})_3$.² Note that in addition to being high in % Cl, the analysis showed % C and % H values lower than theory for green 2. Values of % C, % H, and % Cl calculated for an increasing mole fraction of $\text{MoCl}_3(\text{PMe}_2\text{Ph})_3$ (yellow 3)

(15) Ingram, J. C.; Nebesny, K. W.; Pemberton, J. E. *Appl. Surf. Sci.* 1990, 44, 279.

Table II. 500-MHz ¹H NMR Data (Italicized Resonances Due to Paramagnetic Yellow 3)

		δ, ^a ppm (² J _{H-P} , Hz)					
		methyl			phenyl		
blue 1	this work	1.196 d ^b (8.6)	1.703 t (4.1)	1.905 t (4.0)	7.06 m	7.33 m	7.52 m
	ref 2 ^c	1.23 d	1.73 t	1.93 t			
green 2	this work	-40.5 br	-22.0 br	1.207 d	1.713 t	1.915 t	7.07 m 7.34 m 7.53 m
yellow 3	this work	-40.5 br	-22.4 br				7.9 s 9.1 s 9.4 s 11.2 s
PMe ₂ Ph ^e	this work	1.31 d (0.716)			7.28 m	7.34 m	7.45 m

^a Relative to residual CHCl₃. ^b br ≡ very broad peak, d ≡ doublet, m ≡ complex multiplet, s ≡ singlet, t ≡ triplet. ^c Collected at 60 MHz. ^d An extremely broad signal (11.3–12.5 ppm). ^e Free phosphine/CDCl₃ solution.

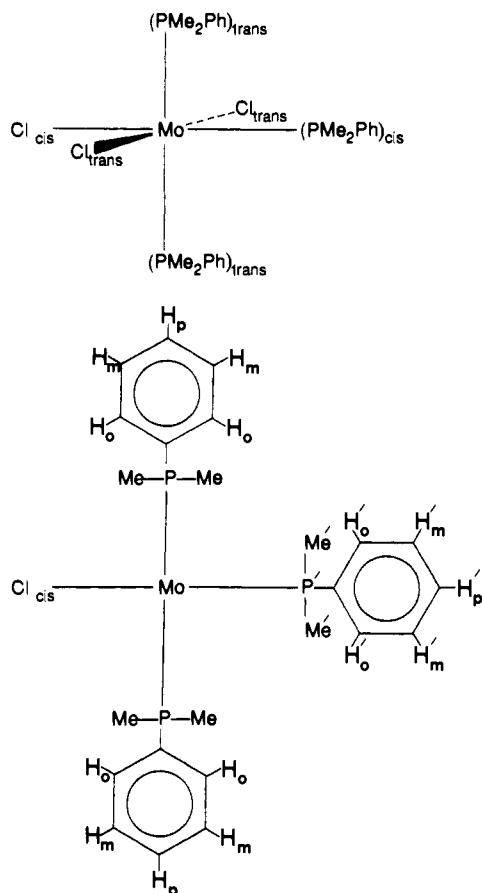


Figure 2. Schematic diagram of *mer*-MoCl₃(PMe₂Ph)₃ (3), emphasizing the number and types of protons seen in the ¹H NMR spectrum. The *cis* and *trans* designations in the peak assignments refer to the methyl or phenyl protons of the unique *cis* phosphine (primed) and the two equivalent *trans* phosphines (unprimed).

in a mixture of MoCl₃(PMe₂Ph)₃ and MoOCl₂(PMe₂Ph)₃ show this same trend of increasing % Cl and decreasing % H and % C. From the data of Table I, the present sample of green 2 is estimated to contain a mole fraction of 0.30 ± 0.10 of yellow 3.

NMR Spectra. The 500-MHz ¹H NMR spectra of blue 1 and green 2 indicated the same multiplicity pattern and similar chemical shifts for the methyl protons of the PMe₂Ph ligands as were previously reported for data collected at 60 and 100 MHz (Figure 1A,B, Table II).^{2,16,17} However, at 500 MHz, the green 2 spectrum had additional peaks assignable to yellow 3. Parkin et al. first examined¹¹ the spectrum of yellow MoCl₃(PMe₂Ph)₃ (3) in the region +10 to -30 ppm to confirm the presence of yellow 3 in the crystals used for X-ray diffraction studies. The present ¹H NMR spectrum of the paramagnetic yellow 3 (Figure 1C,D) showed five characteristic peaks in the region +7.5 to +12 ppm

Table III. Infrared Data (150–500 cm⁻¹)

blue 1		green 2		yellow 3	
this work	ref 2	this work	ref 2	this work	ref 13
484 s		490 s		490 sh	
		482 s		487 s	
				480 s	
435 w		438 w		438 w	
417 m		418 s		418 m	
		411 sh		410 m	
		382 vw		382 vw	
350 w		358 w			
		316 s	310 m	315 s	315 vs
303 w	308 w	301 s	304 m	300 s	300 s
	291 vs ^a	290 vw		291 sh	290 sh
280 s		280 s	285 vs ^a	276 w ^c	277 m
258 vw		258 vw			
243 m	247 s ^b	248 m	248 vs ^b	248 w	
		231 m			
208 w		207 w		208 w	
199 w		199 m		199 w	
178 w	178 m	177 w	183 w	177 w	
		163 w			

^a Assigned to ν(Mo—Cl).² ^b Assigned to δ(Mo=O).² ^c Likely due to ν(M—Cl) by comparison to the analogous Tc complex.^{19b}

and two broad bands at -22.4 and -40.5 ppm. The two broad upfield resonances (Figure 1D) could easily be overlooked in a routine characterization of a sample of green 2 assumed to be completely diamagnetic. Yet, in addition to these two upfield yellow 3 peaks, the green 2 spectrum also showed the characteristic yellow 3 peaks at +7.9, +9.1, +9.4, and +11.2 ppm (Figure 1C), providing additional evidence that green 2 is a mixture of blue 1 and yellow 3.

The 500-MHz spectrum of yellow 3 (Figures 2 and 1C,D) is well resolved and consistent with the recently reported temperature-dependent ¹H NMR (200 MHz) studies of *mer*-MoCl₃(PMe₂Ph)₃.¹⁸ The two broad upfield peaks are likely due to the methyl protons of yellow 3, consistent with earlier assignments of NMR spectra of the paramagnetic complexes *trans*-WCl₄(PMe₂Ph)₂¹⁷ and *mer*-MCl₃(PMe₂Ph)₃ (M = Tc,¹⁹ Re²⁰). Furthermore, the greater intensity of the most upfield resonance (-40.5 ppm) suggests that it is due to the *trans* methyl protons, and the signal at -22.0 ppm results from the *cis* methyl protons. The chemical shifts of the ortho phenyl protons for a large variety of *mer*-ReX₃(ER₂Ph)₃ (E = P, As; R = Me, Et, ⁿPr, ⁿBu)²⁰ and *trans*-MCl₄(ER_{3-n}Ph_n)₃ (M = W,¹⁷ Os,^{20,21} R = Me, Et, ⁿPr, ⁿBu, ⁱBu (M = Os); n = 1, E = P, As; n = 2, E = P) complexes are consistently downfield of their respective para and meta phenyl protons. Partly on this basis, the extremely broad resonance at about 11.3–11.6 ppm is assigned to the combined signals of the unresolved *cis* and *trans* ortho phenyl protons of yellow 3. The remaining four resonances are assigned to the *cis* meta (11.2 ppm), *trans* meta (9.4 ppm), *trans* para (9.1 ppm), and *cis* para (7.9 ppm)

(18) Poli, R.; Mui, H. D. *Inorg. Chem.* **1991**, *30*, 65.(19) (a) Mazzi, U.; De Paoli, G.; Rizzardi, G.; Magon, L. *Inorg. Chim. Acta* **1974**, *10*, L2. (b) Mazzi, U.; De Paoli, G.; Di Bernardo, P.; Magon, L. *Inorg. Chim. Acta* **1976**, *38*, 721.(20) Randall, E. W.; Shaw, D. *J. Chem. Soc. A* **1969**, 2867.(21) Chatt, J.; Leigh, G. J.; Mingos, D. M. P. *J. Chem. Soc. A* **1969**, 1674.(16) Lynden-Bell, R. M.; Mather, G. G.; Pidcock, A. *J. Chem. Soc., Dalton Trans.* **1973**, 715.(17) Butcher, A. V.; Chatt, J.; Leigh, G. J.; Richards, P. L. *J. Chem. Soc., Dalton Trans.* **1972**, 1064.

Table IV. Infrared Data (400–1500 cm⁻¹)

blue 1	green 2	yellow 3	PMe ₂ Ph (free) ^a
1478 m	1481 m	1482 m	1483 m
1435 s ^b	1434 s ^b	1434 s ^b	1432 s ^b
1317 w	1316 w	1317 w	1319 w
1289 m ^c	1293 m ^c	1294 m ^c	1289 m ^c
1277 m	1280 m	1281 m	1274 m
1104 m ^b	1102 m ^b	1102 m ^b	1105 m ^b
998 w ^b	1000 w ^b	1000 w ^b	999 w ^b
		961 m	
		951 s	
941 vs	942 vs		940 vs ^c
908 vs ^c	907 vs ^c	909 vs ^c	895 vs ^c
740 s ^d	740 s ^d	739 s ^d	739 s ^d
695 s ^d	694 s ^d	694 s ^d	694 s ^d
487 s	490 s	489 s	obscured by
419 m	420 m	422, 412 w	NaCl plates

^a Neat, NaCl plates. ^b $\nu(\text{P}-\text{Ph})$.²³ ^c $\nu(\text{P}-\text{CH}_3)$.²³ ^d Phenyl ring bending modes.

phenyl protons. Line widths of the 11.2 and 9.4 ppm peaks are comparable (69 versus 63 Hz, respectively); the peak widths of the 9.1 and 7.9 ppm resonances are also similar (ca. 45 Hz for both). The 2:1 intensities of the 9.4/11.2 ppm pair and of the 9.1/7.9 ppm peaks as well as the line width series of ortho > meta > para (consistent with the proximity of each proton to the Mo(III) center) are in agreement with the above assignments.

Vibrational Spectra. The low-energy infrared spectra (Figure 3A, Table III) clearly showed that differences between the blue and green spectra were attributable to the fact that green 2 was a mixture of blue 1 and yellow 3. Most striking was the region from 350 to 250 cm⁻¹; the three strong bands of green 2 at 316, 301, and 280 cm⁻¹ are an exact superposition of the two bands of yellow 3 at 315 and 300 cm⁻¹ with the single intense band of blue 1 at 280 cm⁻¹. Analogous peaks (310, 304, and 285 cm⁻¹) were reported in the original characterization of green 2.² The green 2 bands near 480 and 418 cm⁻¹ can be also assigned to features from blue 1 and yellow 3. For example, the 490- and 482-cm⁻¹ peaks of green 2 appear to result from the summation of a 484-cm⁻¹ peak from blue 1 and the 490- (shoulder), 487-, and 480-cm⁻¹ peaks from yellow 3. The same argument can be made for the green 2 feature at 418 and 411 (shoulder) cm⁻¹ comprising the 417-cm⁻¹ peak from blue 1 and the 418- and 410-cm⁻¹ peaks from yellow 3. This region of the infrared spectrum provide some of the first evidence for the composite nature of green 2.

The two different M=O bond lengths reported for a pair of distortional isomers suggest two different M=O bond orders.²² It is therefore not surprising that different M=O stretching frequencies have been reported for each of the distortional isomers within a pair.²⁷ However, unique infrared assignment of the $\nu(\text{Mo}=\text{O})$ bands in blue 1 and green 2 is difficult due to the presence of intense ligand $\nu(\text{P}-\text{C})$ bands²³ in the 1000–900-cm⁻¹ region (Figure 3B, Table IV). Each compound's (1, 2, and 3) spectrum has a very strong peak at ca. 908 cm⁻¹. In addition, the spectrum of blue 1 has a single very strong peak at 941 cm⁻¹; yellow 3 has a medium-intensity pair at 961 and 951 cm⁻¹; and green 2 has a very strong peak at 942 cm⁻¹ with features at higher frequencies. Over the same region, the infrared spectrum of free PMe₂Ph has two very strong peaks at 940 and 895 cm⁻¹. Thus it is difficult to confidently assign $\nu(\text{Mo}=\text{O})$ from the infrared spectra. Indeed, the majority of the bands in the "fingerprint" region are common to all three spectra and are directly assignable to phosphine-based vibrations (Figure 3B, Table IV).

Solid-state Raman spectral measurements from 125 to 1625 cm⁻¹ (Figure 4, Tables V and VI) allow identification of the $\nu(\text{Mo}=\text{O})$ frequency and further support the conclusion that green

Table V. Raman Data (620–1625 cm⁻¹)

blue 1	green 2	yellow 3	blue 1	green 2	yellow 3
1590 s	1590 s	1590 s	989 vw	995 sh	989 vw
1576 w	1577 w	1576 w		967 vw	967 vw
1423 vw	1421 vw	1423 vw	943 s ^b	944 s ^b	
	1414 vw	1411 vw		881 vw	881 vw
	1322 vw	1322 vw		856 vw	853 vw
1292 vw	1297 vw	1297 vw		839 vw	838 vw
	1283 vw	1283 vw	754 sh	755 w	752 w
1196 w	1198 vw	1199 vw	748 vw	748 w	745 w
1186 vw	1187 vw			734 w	733 w
1166 vw	1162 vw	1168 w	715 m ^a	714 m ^a	713 m ^a
1135 w	1136 w	1133 w	701 vw	703 vw	701 vw
1111 m	1115 m	1113 m	683 s	684 s	683 s
1032 m	1034 w	1032 w	619 m ^a	619 m ^a	618 m ^a
1002 vs ^a	1003 vs ^a	1003 vs ^a			

^a Ligand bands as internal calibrants. ^b $\nu(\text{Mo}=\text{O})$.

Table VI. Raman Data (125–620 cm⁻¹)

blue 1	green 2	yellow 3	blue 1	green 2	yellow 3
619 s	619 s	618 s	260 m	258 sh	260 w
	500 w	500 w	253 sh	253 m	
488 w	485 vw	487 vw	247 vs		
451 w			232 w	236 vw	238 vw
421 w	421 m	421 m		226 w	226 vw
	415 m	414 m	211 sh	211 sh	211 w
353 m	352 w	352 vw	209 s	208 m	206 w
338 s	338 m	336 w	189 m	195 m	192 m
		326 vw		184 m	
	317 s	313 s		173 m	170 w
309 s	305 vs	304 vs	166 s	164 s	160 s
	295 m	293 m	155 vs	154 vs	
287 s	284 s	284 s	142 vs		147 m
272 m				134 vs	133 vs
268 sh	268 m				

Table VII. Visible and X-ray Photoelectron Data

	λ_{max} , nm	3d _{3/2} ^b	3d _{5/2} ^b
	Blue 1		
this work	396 (265) ^a	611 (67)	233.1
ref 25			233.2
	Green 2		
this work	410 ^c	611 ^c	233.1
	Yellow 3		
this work	355 (1706)	418 (1436)	232.6
ref 25			232.6

^a Molar extinction coefficients in parentheses (L·mol⁻¹·cm⁻¹). ^b Mo 3d binding energies (eV). ^c Molar extinction coefficients would be ambiguous for this mixture.

2 is made up of individual contributions from blue 1 and yellow 3. The relative intensities of the three unshifted ligand peaks at 1003, 715, and 619 cm⁻¹ (labeled with dots in Figure 4) are essentially invariant for all three spectra. The strong blue 1 (943 cm⁻¹) and green 2 (944 cm⁻¹) bands are *absent* in the yellow 3 and the free PMe₂Ph spectra and may be confidently assigned to $\nu(\text{Mo}=\text{O})$. Relative to the common, constant band at 1003 cm⁻¹, the intensity of the green 2 $\nu(\text{Mo}=\text{O})$ band is 38% weaker compared to that of the $\nu(\text{Mo}=\text{O})$ peak of blue 1. This decreased intensity supports green 2 being a 65:35 (blue 1:yellow 3) mixture as determined by UV-vis and XPS spectroscopy (vide infra) and by chemical analysis. The original report² of blue and green MoOCl₂(PMe₂Ph)₃ assigned the infrared bands at 954 (blue) and 944 (green) cm⁻¹ to respective $\nu(\text{Mo}=\text{O})$ frequencies. The Raman data presented here indicate that 943 and not 954 cm⁻¹ is the correct blue 1 Mo=O stretching frequency. The nearly identical $\nu(\text{Mo}=\text{O})$ frequencies (944 ± 1 cm⁻¹) of blue 1 and green 2 preclude bond length differences of the order of 0.1 Å that were originally reported from the crystallographic data.^{4,5,22} Other features of the green 2 Raman spectrum around 734, 415, 317, and 295 cm⁻¹ are also consistent with contributions from yellow 3 in the mixture.

(22) Hardcastle, F. D.; Wachs, I. E. *J. Raman Spectrosc.* 1990, 21, 683 and ref 32 therein.

(23) Silverstein, R. M.; Bassler, G. C.; Morrill, T. C. *Spectrometric Identification of Organic Compounds*, 4th ed.; John Wiley & Sons: New York, 1981; p 170.

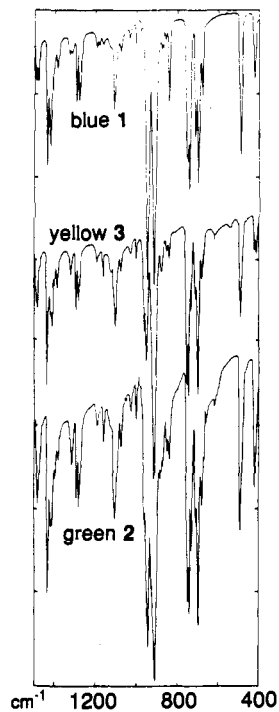
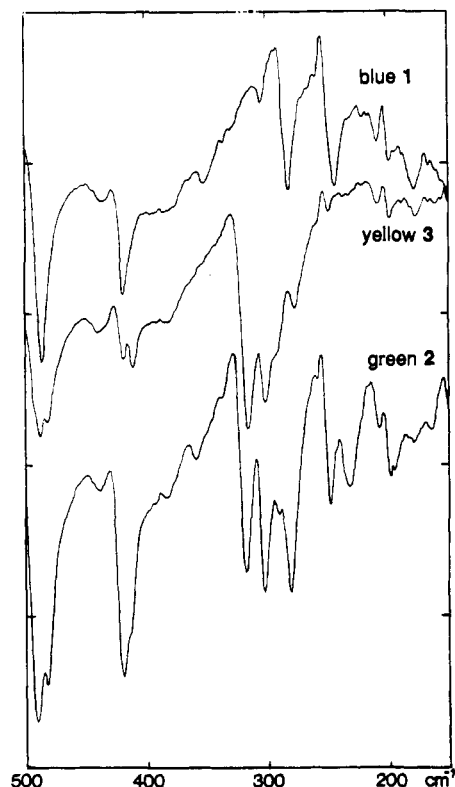


Figure 3. (A, Top) Low-energy infrared spectra (150–500 cm^{-1}) of blue 1, green 2, and yellow 3. Note the common green 2 and yellow 3 peaks in the region 280–350 cm^{-1} . (B, Bottom) Infrared spectra (400–1500 cm^{-1}) of blue 1, green 2, and yellow 3 showing common bands in the “fingerprint” region.

UV-Visible Electronic Spectra. UV-visible electronic spectra provided a rapid and reliable means of quantifying the green mixtures. Although the spectra of blue 1 and green 2 both showed the same $d \rightarrow d$ transition at 611 nm, each had a second transition at 396 and 410 nm, respectively (Figure 5, Table VII). The 410-nm band of green 2 was much more intense (11:1) relative to its 611-nm band than was the 396-nm band of blue 1 (4.5:1). It was the intensity of this 410-nm peak that suggested that green 2 may contain an intensely colored yellow species. Contributions

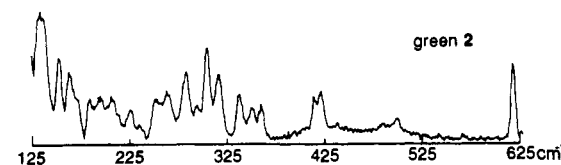
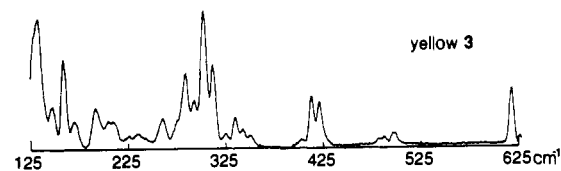
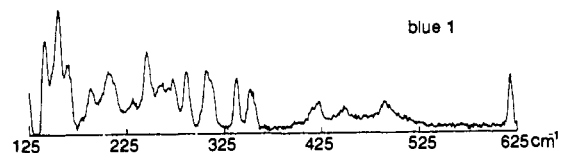
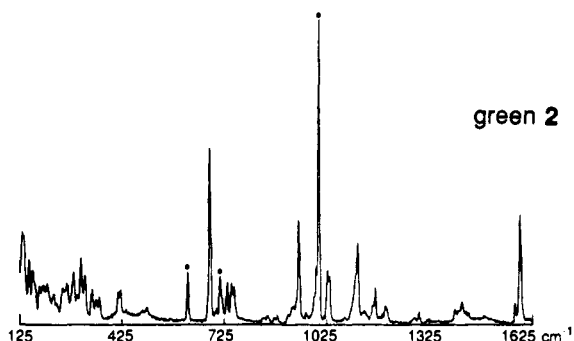
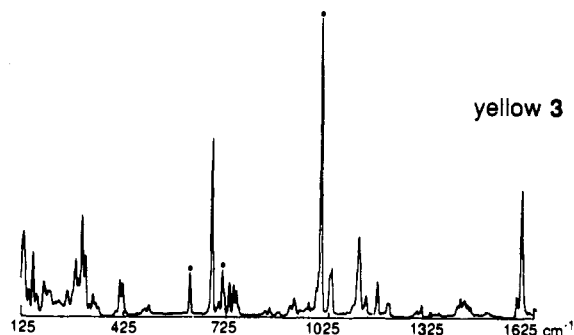
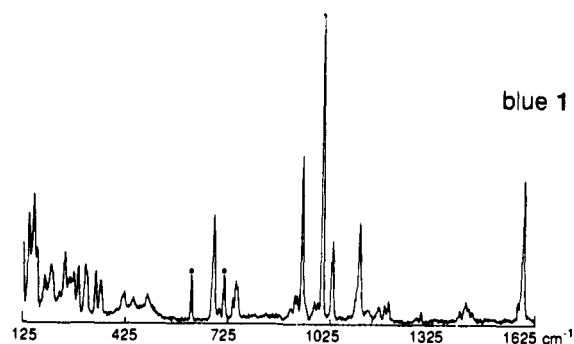


Figure 4. (A, Top) Full Raman spectra (125–1625 cm^{-1}) of blue 1, green 2, and yellow 3. Unshifted PMe_2Ph bands are marked with a dot (\bullet). (B, Bottom) Closeups of the low-energy Raman spectra (125–620 cm^{-1}) of blue 1, green 2, and yellow 3.

from bright yellow 3 explain the appearance and high intensity of the 410-nm peak in the green 2 spectrum. Using the blue 1 and yellow 3 molar extinction coefficients in Table VII, the mole fraction of yellow 3 in our sample of green 2 was determined to be about 0.35. The green 2 spectrum was independently reproduced by mixing the above proportions of blue 1 and yellow 3.

XPS Spectra. Shifts in molybdenum 3d binding energies measurable by X-ray photoelectron spectroscopy (XPS) for compounds with similar coordination environments have been previously exploited in the analysis of systems with multivalent molybdenum centers.²⁴ If green 2 is a composite of Mo(IV) (blue 1) and Mo(III) (yellow 3) species, then the 3d binding energies of the two different metal centers should behave independently of one other, and it should be possible to resolve the Mo 3d XPS spectrum of green 2 into components reflecting the contribution from each oxidation state. The 3d_{3/2}, 3d_{5/2} pair of blue 1 was shifted by about 0.5 eV to higher binding energies relative to yellow 3 (Figure 6, Table VII), as observed previously,^{25,26} and sample degradation under the high-vacuum, X-ray conditions was circumvented by measuring the spectra at -150 °C. The 3d_{3/2}, 3d_{5/2} pair of green 2 appeared at the same energy as that of blue 1, but the peaks were broadened toward lower binding energies relative to those of blue 1 due to the presence of yellow 3. The spectrum of a 70:30 (yellow 3:blue 1) sample prepared by mixing pure yellow 3 and blue 1 showed Mo 3d peaks that were unshifted relative to those of yellow 3 (the major component in this case) but broadened toward higher binding energies due the presence of blue 1. A difference spectrum of green 2 minus 35% of yellow 3 yielded a spectrum that coincided with that originally measured for blue 1 (Figure 6B). These results illustrate the ability of XPS to resolve such intimate mixtures into their constituent contributions. In principle, it would be possible to use the same crystal for an X-ray structure determination and XPS analysis.

Chemistry and Crystallography. One other reported characteristic of distortional isomers is an apparently irreversible conversion of the green isomer (long M=O distance) into its blue counterpart (short M=O distance) in solution.²⁷ The green form of the *cis,mer*-MoOCl₂(PMe₂Ph)₃ system reportedly undergoes such a transformation in ethanol.² On one occasion, the green filtrate from a green 2 synthesis did turn blue over the span of about 10 days at 0 °C, yielding large well-formed crystals of blue 1. However, during the synthesis of yellow 3 in 2-propanol, residue remaining in the yellow filtrate also turned blue within 48 h. It is therefore likely that the reported green to blue "isomerization" in alcohol is simply the oxidation of the yellow Mo(III) component in the green mixture to the blue oxo-Mo(IV) species.

All of the above spectroscopic investigations of green 2 have shown it to be a mixture of blue 1 (MoOCl₂(PMe₂Ph)₃) and yellow 3 (MoCl₃(PMe₂Ph)₃) rather than an example of a "new type of isomerism", i.e. a distortional isomer of *cis,mer*-MoOCl₂(PMe₂Ph)₃, as proposed in 1971.³ The sample described here was approximately 65% blue 1 and 35% yellow 3 (mole percent), but the exact composition varies among preparations.¹¹ How did these mixtures escape detection for 20 years? The original crystal structure of the blue and green forms of the MoOCl₂(PR₂Ph)₃ compounds (R = Me, Et) indicated that the green forms had Mo=O bond lengths that were about 0.1–0.13 Å longer than those in the blue forms.^{3,4,27} Both forms refined satisfactorily for room-temperature structures.²⁸ A later investigation of green 2 (-160 °C, R_w = 0.055) also indicated an unusually long Mo=O distance of 1.80 (2) Å.⁵ Crystallographers are well aware that *intramolecular disorder* between an oxo group and a chloride

ligand cannot normally be crystallographically resolved because the apparent separation between the fractional O and Cl atoms will only be about 0.4–0.7 Å.^{11,29,30} However, it has not been generally realized that the same constraints pertain to *compositionally disordered crystals*. The work of Parkin and co-workers¹¹ clearly demonstrates that mixtures of blue 1 and yellow 3 cocrystallize over a wide range of compositions to give a continuum of Mo=O bond lengths. Thus, an X-ray structure investigation of a crystal of green 2 is often not able to unambiguously distinguish between a mixture of blue 1 and yellow 3 and the hypothesized distortional isomers.⁴² Model crystallographic calculations on mixed W=O/W-Cl compounds show that the number of electron density contours about the oxygen atom is unchanged up to 20 mol % Cl, whereas the apparent M=O bond increases by 0.20 Å.³¹

Although all of the analytical and spectroscopic results for green 2 support the conclusion that it is a mixture of blue 1 and yellow 3, the differences between the characterizations of blue 1 and green 2 are subtle and are apparent only after careful comparison of all of the data for 1, 2, and 3. The Cl analyses for green 2 are somewhat high, but not alarmingly so. The small differences in the ¹H NMR spectra of blue 1 and green 2 would have been undetectable in the original 60-MHz spectra.² The assignment of the infrared bands in the 900–1000-cm⁻¹ region is ambiguous, and the Raman spectra are needed to distinguish the ligand bands from the Mo=O band. The XPS data require careful line shape analysis to reveal that green 2 is a mixture. Of the original data,² only the low-frequency infrared data (350–250 cm⁻¹) and the UV-vis electronic spectra suggest that green 2 is a mixture.³²

Crystallization is usually a purifying process, and yet recrystallization of the green product returns green, apparently homogeneous, crystals. One can envision a free energy change (ΔG_{cryst}) associated with the crystallization process:³³

$$\Delta G_{\text{cryst}} = \Delta H_{\text{cryst}} - T\Delta S_{\text{cryst}}$$

The enthalpy (ΔH_{cryst}) contains contributions from intermolecular interactions as well as intramolecular conformational energies. Now consider the case of blue 1 and yellow 3, which are known to easily cocrystallize. Each molecule contains three bulky meridional dimethylphenylphosphine ligands. The experimental molecular volumes for blue 1 and yellow 3 (699.4 and 703.8 Å³/molecule, respectively) differ by less than 1%.³⁴ Most of their molecular volumes are due to the bulky phosphines, so there may be little difference in polarity between *cis,mer*-MoOCl₂(PMe₂Ph)₃ (blue 1) and *mer*-MoCl₃(PMe₂Ph)₃ (yellow 3). Similar ligand features have been used to explain rotational disorder in M(E)-Cl₃(OPPh₃)₂ (M = Mo, W; E = O, S).³⁵ Therefore, we argue

(29) For example, in the X-ray structure studies of LMoOCl₂ (L = hydrotris(3,5-dimethylpyrazolyl)borate,³⁰ hydrotris(pyrazolyl)borate^{30a}), the observed Mo=O distances are artificially long (2.07–2.27 Å) due to rotational disorder of the MoOCl₂ fragment.

(30) (a) Lincoln, S.; Koch, S. A. *Inorg. Chem.* **1986**, *25*, 1594. (b) Ferguson, G.; Kaitner, B.; Lalor, F. J.; Roberts, G. *J. Chem. Res. Synop.* **1982**, *1*, 6. (c) Marabella, C. P.; Enemark, J. H. Unpublished results.

(31) Desrochers, P. J. Unpublished results.

(32) The original report² of green 2 notes that this material is difficult to separate from a yellow species formulated as 3. However, pure yellow 3 was not prepared until 1976,¹³ five years after the initial proposal of "distortional isomers".³ Other previously known cases of intimate mixtures of oxo and chloro compounds include "violet *trans*-Re(OH)Cl₃(PMe₂Ph)₂" (Chatt, J.; Rowe, G. A. *J. Chem. Soc.* **1962**, 4019), later characterized (Chatt, J.; Garforth, J. D.; Johnson, N. P.; Rowe, G. A. *J. Chem. Soc.* **1964**, 601) by chromatography and infrared, visible electronic, and ¹H NMR spectroscopies to be a mixture of 10–22% *trans*-ReCl₄(PMe₂Ph)₂ (violet) in *trans*-ReOCl₃(PMe₂Ph)₂ (green).

(33) Shriver, D. F.; Atkins, P. W.; Langford, C. H. *Inorganic Chemistry*; W. H. Freeman and Co.: New York, 1990; p 573.

(34) Calculated using unit cell parameters obtained from ref 11.

(35) The origin of the rotational disorder in the complexes MoOCl₃(OPPh₃)₂, WOCl₃(OPPh₃)₂, and WSCl₃(OPPh₃)₂ is described in ref 14 of ref 30a.

(24) Grünert, W.; Stakheev, A. Y.; Feldhaus, R.; Anders, K.; Shpiro, E. S.; Minachev, K. M. *J. Phys. Chem.* **1991**, *95*, 1323.

(25) Chatt, J.; Elson, C. M.; Leigh, G. J. *J. Chem. Soc., Dalton Trans.* **1976**, 1351.

(26) Leigh, G. J.; Bremser, W. *J. Chem. Soc., Dalton Trans.* **1972**, 1216.

(27) Manojlović-Muir, L.; Muir, K. W. *J. Chem. Soc., Dalton Trans.* **1972**, 686.

(28) Blue MoOCl₂(PMe₂Ph)₃: Mo=O = 1.676 (7) Å, refined to a final R_w = 0.062.⁴ Green MoOCl₂(PEt₂Ph)₃: Mo=O = 1.801 (9) Å, refined to a final R_w = 0.081.²⁷

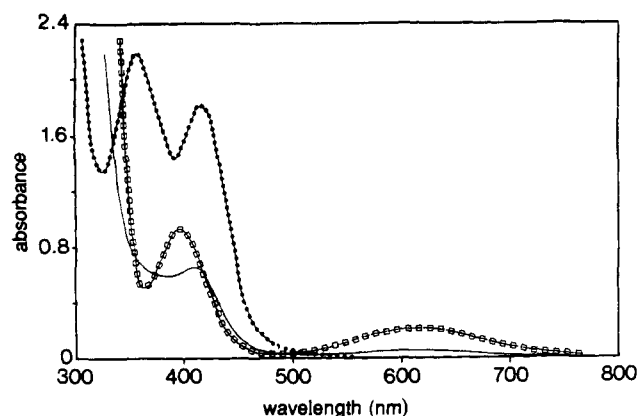


Figure 5. Visible spectra of blue 1 (□), green 2 (—), and yellow 3 (•) in dry acetonitrile. Concentrations: blue 1, 3.80 mM; green 2, 18.5 mg in 25.0 mL; yellow 3, 1.17 mM.

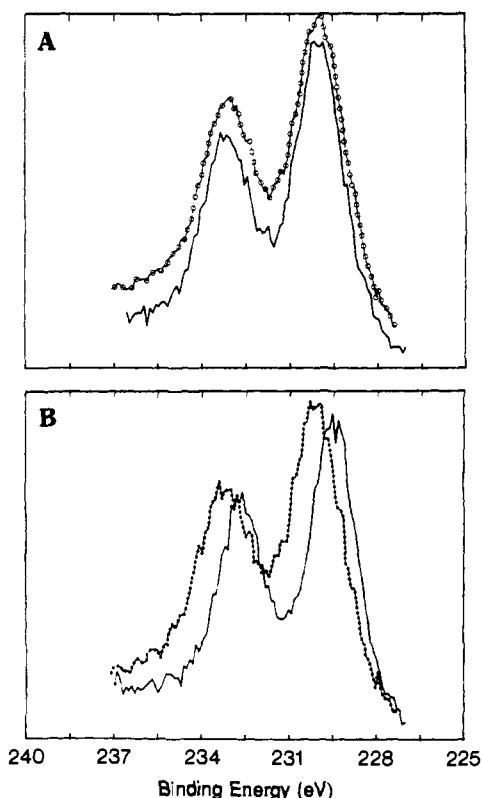


Figure 6. X-ray photoelectron spectra of the molybdenum 3d peaks: A, spectra of blue 1 (—) and green 2 (•); B, spectrum of yellow 3 (—) and a difference spectrum (•) = (green 2) - (0.35)(yellow 3). The peaks of the green-minus-yellow difference spectrum match those of the original blue 1 spectrum.

that the ΔH_{cryst} contributions of these individual molecules are similar and that the increased entropy (ΔS_{cryst}) afforded by the cocrystallization of blue 1 and yellow 3 provides the thermodynamic driving force³³ for the ready formation of the compositionally disordered crystals of green 2.

General Conclusions on Distortional Isomers. The results of Parkin and co-workers¹¹ and the spectroscopic results reported here show that the blue and green forms of $\text{MoOCl}_2(\text{PMe}_2\text{Ph})_3$ are not "distortional isomers". Rather, the green form is a mixture of the blue *cis,mer-MoOCl₂(PMe₂Ph)₃* and the yellow *mer-MoCl₃(PMe₂Ph)₃*. The concept of distortional isomerism has been invoked several times since 1971^{7-9,36,37} to explain other examples

of compounds with the same apparent molecular formulas and stereochemistries but with different colors and different bond lengths. Distortional isomerism is even discussed in a recent undergraduate inorganic chemistry textbook.³⁸ However, the recent structural¹¹ and spectroscopic results for the original Butcher and Chatt system² also call into question the validity of the other postulated examples^{7-9,36} of distortional isomerism.

All transition-metal systems claimed to exhibit distortional isomerism, with the exception of the aquooxocyanomolybdate examples,³⁶ possess three important common characteristics. All have terminal metal-oxo or -sulfido units; all have terminal halogen ligands; and all have bulky organic amine or phosphine ligands. In light of the current evidence for cocrystallization, it seems likely that all of these examples are actually mixtures in which the terminal oxo or sulfido group is replaced by a halogen atom in a fraction of the molecules. For example, consider the recently reported yellow and green distortional isomers of $\text{NbOCl}_3(\text{PMe}_2\text{Ph})_3$,^{8a,c} The oxygen atom in $\text{NbOCl}_3(\text{PMe}_2\text{Ph})_3$ caps the face of the three PMe_2Ph ligands, a coordination geometry nearly identical to that of the structurally characterized³⁹ green Nb(IV) species $\text{NbCl}_4(\text{PMe}_2\text{Ph})_3$, which has a chlorine capping the face of the three phosphines. The unusually long Nb=O bond of the one isomer of $\text{NbOCl}_3(\text{PMe}_2\text{Ph})_3$ may well be an artifact of compositional disorder in a cocrystallized mixture of $\text{NbOCl}_3(\text{PMe}_2\text{Ph})_3$ and $\text{NbCl}_4(\text{PMe}_2\text{Ph})_3$.^{8c} Our model X-ray calculations³¹ on blue and green $[\text{WOCl}_2]\text{PF}_6$ suggest that compositional disorder accounts for the unusual W=O and W-Cl bond lengths^{7b} in this pair. Experimental studies of the latter system are currently in progress.⁴⁰

Finally, we note that, for the system investigated in this research, the minor yellow *mer-MoCl₃(PMe₂Ph)₃* component (3) in blue *cis,mer-MoOCl₂(PMe₂Ph)₃* (1) alters the color of the mixed crystal to green and evidences itself as a paramagnetic component in the ¹H NMR samples. Similar compositionally disordered crystals may exist for systems in which both components have the same color and are in the same magnetic state.⁴¹ Such disordered systems can be extremely difficult to detect but could have a profound effect on the current understanding of metal-ligand distances determined from X-ray crystallography.

Acknowledgment. We thank Dr. S. Sperline for his assistance with the FT-IR measurements. We also acknowledge helpful discussions with Drs. M. Bruck, B. Haymore, L. Manojlović-Muir, J. Mayer, L. Mink, K. W. Muir, G. Parkin, S. Roberts, F. A.

(38) Miessler, G. L.; Tarr, D. A. *Inorganic Chemistry*; Prentice Hall: Englewood Cliffs, NJ, 1991; p 369.

(39) Cotton, F. A.; Diebold, M. P.; Roth, W. J. *Polyhedron* **1985**, *4*, 1103.

(40) Desrochers, P. J.; Wiegardt, K.; Enemark, J. H. Research in progress.

(41) (a) Haymore, B. L. Private communication. (b) Yoon, K.; Parkin G. *J. Am. Chem. Soc.*, in press.

(42) Note Added in Proof. Subsequent to the spectroscopic study reported here, we have investigated the X-ray structure of a representative crystal (0.4 × 0.2 × 0.1 mm) from the same sample of green 2 sealed in a glass capillary under nitrogen, using a CAD-4 diffractometer (Mo K α radiation) at 21 °C. Several ω scans through small-angle reflections revealed ω half-height widths of 0.25–0.35°. The monoclinic unit cell ($a = 16.090$ (2) Å, $b = 10.384$ (1) Å, $c = 18.039$ (2) Å; $\beta = 113.85$ (1)°; $Z = 4$; $P2_1/c$) is isomorphous with the previous green 2 structure⁵ and with yellow 3.¹¹ The structure of the $\text{MoCl}_2(\text{PMe}_2\text{Ph})_3$ fragment common to 1 and 3 was well determined from 4049 observed reflections ($2\theta \leq 50^\circ$, $d_{\text{min}} = 0.84$ Å); approximately half of the hydrogens were visible in the final difference maps. Refinement as pure 1 with a single oxygen position ($R_w = 0.0758$) gave Mo-O = 2.125 (2) Å and an abnormally small thermal parameter. This distance is consistent with previous results¹¹ for green mixtures that were created to be about 30 mol % yellow 3. Refinement of a model that included coordinates for both an O atom of 1 and a Cl atom of 3 with variable occupancy factors showed several correlation coefficients of ca. 0.7 but gave the best fit to the data ($R_w = 0.0548$), converging to 44.2 (1) mol % yellow 3 with Mo-O = 1.728 (4) Å ($B = 3.85$ (9) Å²), Mo-Cl = 2.270 (9) Å ($B = 4.29$ (4) Å²), and an apparent O...Cl distance of 0.634 (5) Å. Although the derived Mo-O length is longer than in blue 1 and the Mo-Cl length is shorter than in yellow 3, the bond angles for the respective blue 1 and yellow 3 components were essentially the same as those in the pure crystals of these materials.¹¹ Thus, our crystallographic results and the chemical and spectroscopic data for the present sample of green 2 are consistent with it being a mixture that contains a 0.30–0.45 mole fraction of yellow 3. Complete details will appear in the Ph.D. dissertation of P.J.D.

(36) Wiegardt, K.; Backes-Dahmann, G.; Holzbach, W.; Swiridoff, W. *J. Weiss, J. Z. Anorg. Allg. Chem.* **1983**, *499*, 44.

(37) Cotton, F. A.; Diebold, M. P.; Roth, W. J. *Inorg. Chem.* **1987**, *26*, 2848.

Walker, K. Wiegardt, and K. Yamanouchi. Special thanks are expressed to Dr. Parkin for preprints of refs 11 and 41b and to Prof. M. Hall for a preprint of ref 10b. This work was supported in part by the National Institutes of Health (Grants GM37773 to J.H.E. and GM18865 to T.M.L.), the Materials Characteri-

zation Program of the University of Arizona, and the North Atlantic Treaty Organization (Grant 86/0513).

Registry No. MoOCl₂(PMe₂Ph)₃, 30134-06-6; MoCl₃(PMe₂Ph)₃, 36926-67-7.

A Highly Reactive Functional Model for the Catechol Dioxygenases. Structure and Properties of [Fe(TPA)DBC]BPh₄

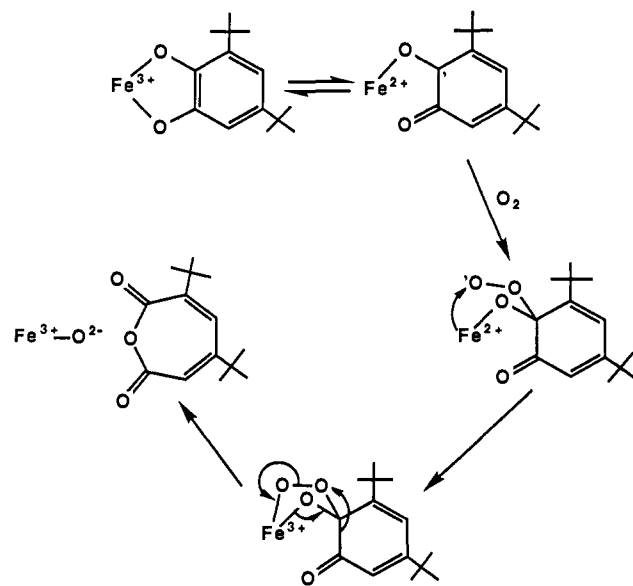
Ho G. Jang, David D. Cox, and Lawrence Que, Jr.*

Contribution from the Department of Chemistry, University of Minnesota, Minneapolis, Minnesota 55455. Received May 2, 1991

Abstract: [Fe^{III}(TPA)DBC]BPh₄, a new functional model for the catechol dioxygenases, has been synthesized, where TPA is tris(2-pyridylmethyl)amine and DBC is 3,5-di-*tert*-butylcatecholate dianion. The TPA complex reacts with O₂ within minutes to afford intradiol cleavage, in 98% yield, which is the highest conversion observed of all [Fe(L)DBC] complexes studied. More interestingly, the TPA complex is the fastest reacting of all the [Fe(L)DBC] complexes studied. Kinetic studies of the reaction of the complex with 1 atm of O₂ in DMF under pseudo-first-order conditions show that the TPA complex reacts approximately three orders of magnitude faster than the corresponding NTA complex, where NTA is *N,N*-bis(carboxymethyl)glycine. Both the high specificity and the fast kinetics can be associated with the high Lewis acidity of the ferric center in the TPA complex. To investigate the factors determining reactivity, we have solved the crystal structure of [Fe(TPA)DBC]BPh₄ (space group P $\bar{1}$, $a = 12.464(5)$ Å, $b = 13.480(6)$ Å, $c = 15.980(8)$ Å, $\alpha = 85.11(4)^\circ$, $\beta = 83.96(4)^\circ$, $\gamma = 70.76(4)^\circ$, $V = 2517(4)$ Å³, $Z = 2$, $R = 0.054$ and $R_w = 0.063$). Compared with other complexes in the [Fe(L)DBC] series, the iron-catecholate interaction in the TPA complex is significantly stronger, resulting in the enhanced covalency of the metal-catecholate bonds and low-energy catecholate LMCT bands. The enhanced covalency is reflected by the isotropic shifts exhibited by the DBC protons, which indicate increased semiquinone character. The greater semiquinone character in the TPA complex correlates well with its high reactivity toward O₂. These trends provide substantial evidence for the substrate activation mechanism proposed for the oxidative cleavage of catechols.

The catechol dioxygenases catalyze the oxidative cleavage of catechols and serve as part of nature's strategy for degrading aromatic molecules in the biosphere.¹ Significant progress²⁻⁷ has been made in understanding the active site of the intradiol cleaving enzymes and is highlighted by the recent solution of the crystal structure of native protocatechuic 3,4-dioxygenase.⁸ Functional mimics for these enzymes have also been developed since the flexibility in ligand design allows a systematic study of the important factors affecting reactivity as well as reaction mechanism.⁹⁻¹² In our biomimetic efforts, we have focused on obtaining structurally characterized complexes capable of oxidative cleavage activity.^{10,12} By studying a series of [Fe^{III}(L)DBC]¹³ complexes

Scheme 1



where L is a tetradentate tripodal ligand, we have demonstrated a direct correlation between the rate of oxidative cleavage of the bound catecholate ligand and the Lewis acidity of the ferric center,

(1) For recent reviews of these enzymes, see: Que, L., Jr. *Adv. Inorg. Biochem.* **1983**, *5*, 167. Que, L., Jr. *J. Chem. Educ.* **1985**, *62*, 938. Que, L., Jr. In *Iron Carriers and Iron Proteins*; Loehr, T. M., Ed.; VCH Publishers: New York, 1989; p 467.

(2) (a) Whittaker, J. W.; Lipscomb, J. D.; Kent, T. A.; Münck, E. *J. Biol. Chem.* **1984**, *259*, 4466. (b) Kent, T. A.; Münck, E.; Pyrz, J. W.; Widom, J.; Que, L., Jr. *Inorg. Chem.* **1987**, *26*, 1402.

(3) (a) Que, L., Jr.; Heistand, R. H., II; Mayer, R.; Roe, A. L. *Biochemistry* **1980**, *19*, 2588. (b) Que, L., Jr.; Epstein, R. M. *Biochemistry* **1981**, *20*, 2545.

(4) Whittaker, J. W.; Lipscomb, J. D. *J. Biol. Chem.* **1984**, *259*, 4487.

(5) (a) Felton, R. H.; Barrow, W. L.; May, S. W.; Sowell, A. L.; Goel, S. *J. Am. Chem. Soc.* **1982**, *104*, 6132. (b) True, A. E.; Orville, A. M.; Pearce, L. L.; Lipscomb, J. D.; Que, L., Jr. *Biochemistry*, **1990**, *29*, 10847.

(6) Que, L., Jr.; Lauffer, R. B.; Lynch, J. B.; Murch, B. P.; Pyrz, J. W. *J. Am. Chem. Soc.* **1987**, *109*, 5381.

(7) (a) Bull, C.; Ballou, D. P.; Otsuka, S. *J. Biol. Chem.* **1981**, *256*, 12681.

(b) Walsh, T. A.; Ballou, D. P.; Mayer, R.; Que, L., Jr. *J. Biol. Chem.* **1983**, *258*, 14422.

(8) Ohlendorf, D. H.; Lipscomb, J. D.; Weber, P. C. *Nature* **1988**, *336*, 403.

(9) (a) Funabiki, T.; Tada, S.; Yoshioka, T.; Takano, M.; Yoshida, S. *J. Chem. Soc., Chem. Commun.* **1986**, 1699. (b) Funabiki, T.; Mizoguchi, A.; Sugimoto, T.; Tada, S.; Tsuji, M.; Yoshioka, T.; Sakamoto, H.; Takano, M.; Yoshida, S. *J. Am. Chem. Soc.* **1986**, *108*, 2921. (c) Funabiki, T.; Konishi, T.; Kobayashi, S.; Mizoguchi, A.; T. M.; Takano, M.; Yoshida, S. *Chem. Lett.* **1987**, 719.

(10) Que, L., Jr.; Kolanczyk, R. C.; White, L. S. *J. Am. Chem. Soc.* **1987**, *109*, 5373.

(11) Cox, D. D.; Benkovic, S. J.; Bloom, L. M.; Bradley, F. C.; Nelson, M. J.; Que, L., Jr.; Wallick, D. E. *J. Am. Chem. Soc.* **1988**, *110*, 2026.

(12) Cox, D. D.; Que, L., Jr. *J. Am. Chem. Soc.* **1988**, *110*, 8085.

(13) Abbreviations: NTA, *N,N*-bis(carboxymethyl)glycine; PDA, *N*-(carboxymethyl)-*N*-(2-pyridylmethyl)glycine; BPG, *N,N*-bis(2-pyridylmethyl)glycine; TPA, tris(2-pyridylmethyl)amine; DBCH₂, 3,5-di-*tert*-butylcatechol; py, pyridine.